

# Impact of Collector Array Orientation on the Performance of a Flat Collectors Field for Middle-Temperature Applications

Eliana Gaudino<sup>1,2\*</sup>, Alessandro Vitaliano Anacreonte<sup>1,2</sup>, Antonio Caldarelli<sup>2</sup>, Paolo Strazzullo<sup>1,2</sup>, Marilena Musto<sup>1,2</sup>, Nicola Bianco<sup>1,2</sup>, Francesco Di Giamberardino<sup>3</sup>, Rosario Iameo<sup>4</sup>, Vittorio G. Palmieri<sup>3</sup>, Roberto Russo<sup>2</sup>

1 Industrial Engineering Department, University of Napoli "Federico II", Piazzale Vincenzo Tecchio, 80, 80125 Napoli, Italy

2 Institute of Applied Sciences and Intelligent Systems, National Research Council of Italy, via Pietro Castellino 111 80131 Napoli, Italy

3TVP Solar SA, 10 rue de Pré-de-la-Fontaine ZIMEYSA 1242 Satigny (GE) Switzerland

4 TRESOL Srl, Pianodardine, Avellino, Italy  
(eliana.gaudino@isasi.cnr.it)

## ABSTRACT

The orientation of solar collector arrays significantly influences the efficiency and performance of solar thermal systems. However, in some instances, practical limitations may prevent the optimal orientation of these collector arrays. This research investigates the performance of a field of High Vacuum Flat Collectors (HVFPCs) under suboptimal conditions. Our test facility features 25 arrays located on both sides of a building's roof. Each array forms a 6° angle with the horizontal plane. Of these, four panels are on the east-facing surface, and three are on the west-facing surface. All collectors within the arrays have a tilt angle of 15° and an azimuth angle of 0°. We began performance assessments using a single pyranometer placed between the two roof sides to gauge solar irradiation. Later, we used two pyranometers one on each roof side. Both had identical tilt and azimuth as the collectors, ensuring independent irradiation measurements. When comparing these measurements to numerical results from a dynamic simulation, we discovered that a comprehensive plant performance evaluation must account for the varied orientations of collectors in the arrays. These results underscore the need to consider collector orientation's impact on performance, even if ideal orientations are unattainable due to installation challenges. Understanding how non ideal collector array orientation affects system efficiency leads to improved flow rate regulation techniques, optimizing performance and energy use.

**Keywords:** solar thermal, solar energy, collector orientation, solar field performance measurements, dynamic simulation.

## NOMENCLATURE

### Abbreviations

$A_c$	Collector surface (m <sup>2</sup> )
$c_p$	HTF Specific Heat (J/kgK)
FPC	Flat Plate Collector
$G$	Solar irradiation (W/m <sup>2</sup> )
HTF	Heat Transfer Fluid
HVFPC	High Vacuum Flat Plate Collector
$\dot{m}$	HTF mass flow rate (kg/s)
$N_c$	Number of collectors of the field
$T_{amb}$	Ambient Temperature (°C)
$T_m$	Average HTF Temperature between field inlet & outlet

### Symbols

$\beta$	Tilt angle (°)
$\Delta T$	HTF Temperature difference between field outlet and inlet (°C)
$\gamma$	Azimuth angle (°)
$\theta$	Angle of Incidence (°)

## 1. INTRODUCTION

The orientation of solar collector arrays is fundamental in harnessing solar energy efficiently for various applications [1].

Solar collectors, particularly Flat Plate Collectors (FPCs), are designed to capture and convert solar radiation into usable thermal energy [2]. The optimal orientation of these collectors significantly impacts the performance and overall system efficiency. Typically, the orientation of a solar collector and its surface's relation to the Sun are characterized by three angles [3]: Angle of Tilt ( $\beta$ ) is the angle between the plane of the collector (or aperture) and the horizontal; Azimuth angle ( $\gamma$ ) is the horizontal angle between exact south and the direction the surface of the device is facing; and the Angle of Incidence ( $\theta$ ) that is the angle between the vector perpendicular to the collector plane, called the normal of the plane, and the projection of the Sun's central beam to the collector surface. The geographical location and the specific application requirements determine the ideal orientation for solar collectors. In the northern hemisphere, collectors are typically oriented towards the south. This alignment allows the collectors to maximize their exposure to the sun's rays throughout the day, optimizing energy absorption and conversion. The orientation of FPCs affects the angle  $\theta$ , which directly influences the amount of energy captured. When collectors are tilted at an angle equal to the latitude of the installation site [4], they receive solar radiation more perpendicularly, maximizing energy absorption. However, deviations from this optimal  $\beta$  often occur due to practical constraints, such as roof slope limitations, architectural considerations, or aesthetic requirements. The impact of collector orientation on system performance also affects the distribution of thermal energy within the system [5], influencing factors such as the uniformity of heat transfer fluid (HTF) flow and the overall system temperature distribution. These factors impact the heat transfer efficiency. The availability of direct and diffuse solar radiation throughout the day further complicates the determination of optimal orientation. The angle of incidence for direct radiation varies with the sun's position, while diffuse radiation remains evenly distributed.

This study measures and analyzes a TVP-Solar MT-Power High Vacuum Flat Collectors field, where the collectors are installed on the two sides of a building roof at a specific angle. The field comprises multiple collector arrays with east- and west-facing panels. Initially, the field performance of the HVFPCs was evaluated using a setup with a singular pyranometer measuring solar irradiation across the field. A subsequent measurement campaign introduced an additional pyranometer, allowing for individualized solar irradiation measurements on each roof side.

The comparison of measurements with numerical results obtained with a simulation model of the field implemented in Simulink will help determine the appropriate experimental setup configuration. Comparing these measurements with numerical results from a Simulink simulation model will guide the determination of the most suitable experimental setup configuration. Through this study, we aim to assess the effects of non-optimal orientations on energy yield and efficiency and explore the significance of acknowledging different collector orientations within arrays when managing flow rate.

## METHODS

### 2.1 TVP-Solar MT-Power High Vacuum Flat Plate Collectors

Before describing the solar field analyzed, it is important to give some information about the main component of the analyzed plant.

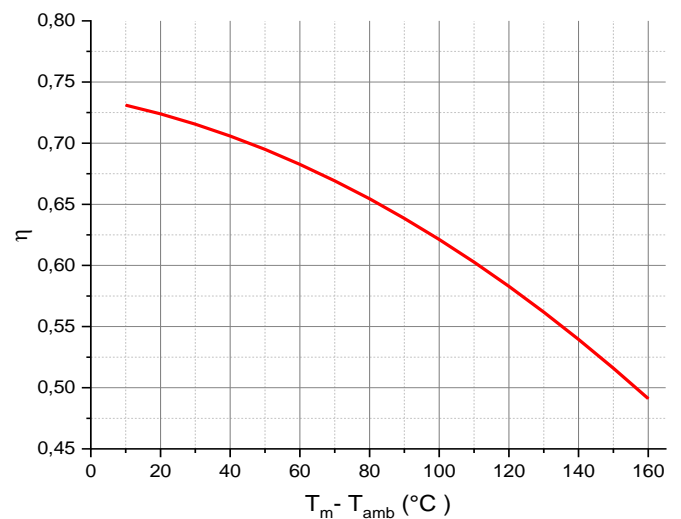


Figure 1 MT-power HVFPC thermal efficiency curve as certified by the Solar Keymark.

The MT-Power V4 HVFPC, manufactured by TVP Solar, is a high-performance solar thermal collector designed for mid-temperature applications (up to 180°C) and superior efficiency. Its innovative design includes a high-vacuum insulation panel and a selective coating on the absorber surface [6]. This design allows for minimal heat loss and efficient absorption of solar radiation, resulting in improved overall performance [7]. The efficiency of the MT-Power collector is certified by the solar Keymark and represented in Fig. 1. The certified efficiency curve is reported as a function of the difference between operating and ambient temperature ( $T_{avg} - T_{amb}$ ).

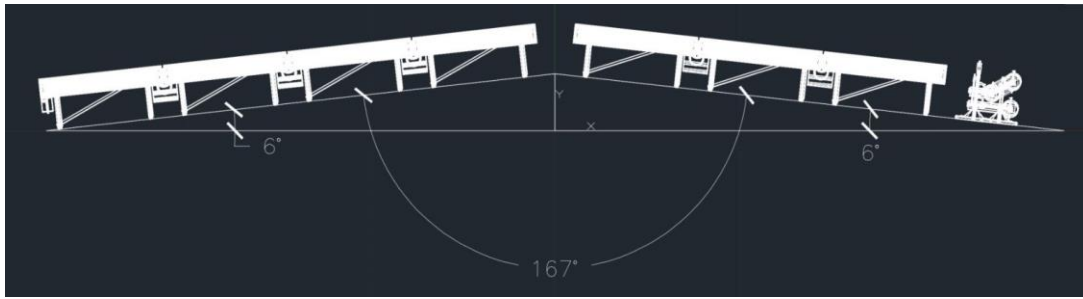


Figure 2 Frontal section of one array of collectors of the solar field mounted on the roof with a  $6^\circ$  angle on both sides.

The curve is obtained at perpendicular illumination conditions with an irradiation value of  $G=950 \text{ W/m}^2$ .

Compared to other commercially available solar collectors, the MT-Power demonstrates excellent conversion efficiencies, particularly at low irradiances ( $< 500 \text{ W/m}^2$ ) [8]. The MT-Power's ability to maintain high conversion efficiencies even under low irradiance conditions is advantageous when the collectors may experience reduced solar radiation due to shading, suboptimal orientations, or other environmental factors. In the analyzed case, where the roof's inclination limits the uniform illumination of the collectors, the MT-Power's performance at low irradiances becomes particularly valuable.

### 2.1 Solar Field Description

The analyzed solar field comprises two main parts. The first component, located on the roof, consists of 175 High Vacuum Flat Plate Collectors (HVFCs) manufactured by TVP Solar Company [8]. The field is divided into 25 arrays, each containing seven panels. Within each array, four panels are mounted on the east-facing side of the roof, while the remaining three are situated on the west-facing side. The two sides of a building roof form an angle of  $6^\circ$  with the horizontal plane as shown in Fig. 2. The collectors in the arrays have a  $\beta$  of  $15^\circ$  and  $\gamma$  equal to  $0^\circ$ .



Figure 3 Solar Field test-facility on the roof of TVP-Solar company

The collectors are connected in series by hose connectors and are interconnected through supply and return pipelines (see Fig. 3). Notably, in addition to the supply and return pipes, there is a third pipe that serves as a pressure equalizer. This pipe balances the pressure between the two main pipes to prevent flow reversal in certain rows due to pressure differentials. Furthermore, a vent valve is incorporated into the system to release excess pressure if necessary.

The solar field follows a single side module format, whereby the pipelines run laterally through the field. At ground level, the thermal block consists of two subsystems. Subsystem 1 primarily includes a pressurization pump, an expansion vessel, and a buffer tank. These components work together to adjust the flow rate and to maintain the system pressure within the desired range of 0.6-1.0 MPa. This pressure range prevents any potential evaporation.

Since the facility currently lacks a designated application, Subsystem 2 is crucial when the Heat Transfer Fluid (HTF) achieves its target temperature. In this case, the HTF is channeled for cooling. This subsystem is equipped with a dry cooler and an electromagnetic three-way valve. When the HTF's temperature at the field outlet surpasses the set threshold, the valve redirects it to the dry cooler for cooling before recirculation.

### 2.2 Performance measurement procedure

The objective of the performance measurements carried out on the solar field is to monitor its daily productivity and field efficiency.

Water was selected as HTF, and the set-point temperature for each measurement day was determined accordingly. To evaluate the field's performance, we monitored several variables, including: HTF temperature at the inlet and outlet of the solar field, HTF temperature at the inlet and outlet of the dry cooler, HTF flow rate at the inlet of the solar field and at the inlet of the dry cooler, Solar irradiation, and ambient temperature.

Initially, the measurements campaign focused on monitoring solar irradiation using a single pyranometer installed in the middle of the roof (neglecting the 6° additional inclination to the east and the west). A fixed HTF flow rate of 8 m<sup>3</sup>/h was maintained.

The measurement results were then compared with the numerical results obtained from a simulation model of the field implemented in Simulink [9]. However, the discrepancies between the measured and simulated results prompted a repeat of the measurements campaign. In the subsequent measurements campaign, solar irradiation was monitored separately on each side of the building roof using two pyranometers, as depicted in Fig. 4. Additionally, the flow rate regulation took into account the average value of the irradiation measured by the two pyranometers.

This adjustment aimed to incorporate the localized variations in solar irradiation across the roof.



Figure 4 Arrangement of the two pyranometers for the second measurements campaign parallel to the panel surface

In both cases, the measurements were conducted when  $G \geq 150 \text{ W/m}^2$  to capture the full range of solar illumination. This extended timeframe was chosen because the orientation of the collector arrays (mounted on the east-facing and west-facing sides of the roof) results in varying illumination levels during the early part of the day and at the end.

By measuring throughout the entire daylight period, the differences in solar radiation received by the collectors due to their different orientations can be accurately assessed.

The results obtained from both measurement configurations and the considerations derived from the analysis will be presented in the results section.

### 3 RESULTS AND DISCUSSION

The following section will compare the experimental results of both measurement campaigns with numerical results.

#### 3.1 Performance measurements with single pyranometer and comparison with numerical results.

Figure 5 displays the measurement results obtained during a single day of the measurement campaign, where solar irradiation was monitored using a single pyranometer positioned in the middle of the building roof. The chosen day for presenting the results is 18 March 2023, with a set-point temperature of 95 °C, a typical application temperature for a solar thermal field. In Fig. 5a), the acquired weather conditions are depicted. This includes the solar irradiation  $G$  measured by the single pyranometer and the ambient temperature  $T_{\text{amb}}$ .

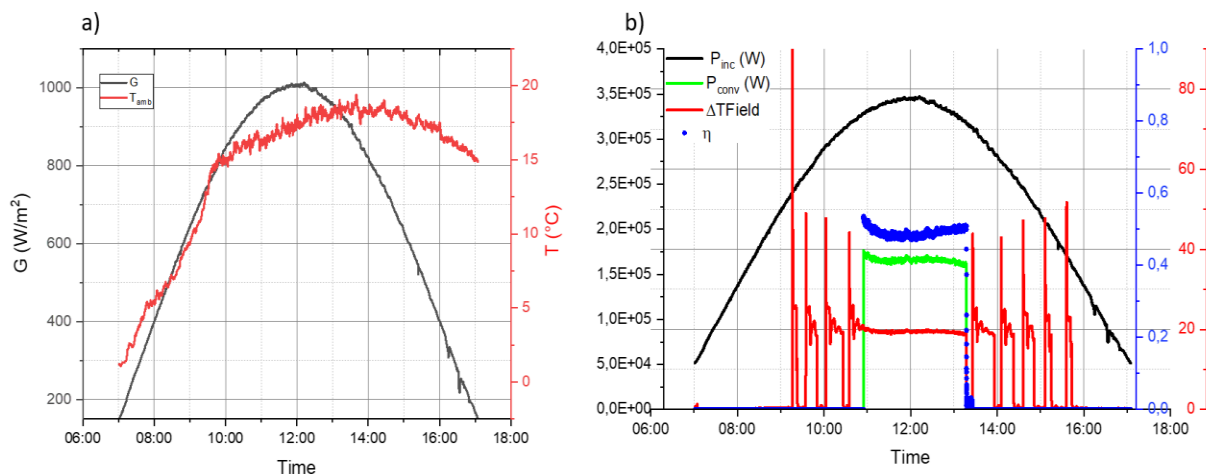


Figure 5 a) 18/03/2023 acquired weather data, solar irradiation (black line, left scale) and ambient temperature (red line right scale) b) Measured field performance parameters with a set point temperature equal to 95 °C: incident power, produced power,  $\Delta T$  and efficiency.



In Fig. 5b), the performance parameters of the solar field are presented.

The temperature difference ( $\Delta T$ ) represents the increment in HTF temperature achieved by the solar field. The observed oscillations in  $\Delta T$  are attributed to incorrect flow rate and dry cooler power regulation.  $P_{inc}$  (W) represents the solar power incident on the surface of the collectors comprising the solar field. It is calculated using the formula (1):

$$P_{inc} = G * A_c * N_c \quad (1)$$

$P_{conv}$  (W) represents the amount of power the solar field converts while maintaining the set-point temperature. It is computed using the formula:

$$P_{conv} = \dot{m} * c_p * \Delta T \quad (2)$$

$\eta$  is the field efficiency and in the graph is represented for a set point operating temperature of 95 °C and ( $T_{avg} - T_{amb}$ ) of approximately 70 °C. It is computed using the formula:

$$\eta = \frac{P_{conv}}{P_{inc}} \quad (3)$$

The daily results obtained from the measurements campaign were compared with the numerical results obtained from a simulation model of the solar field implemented in Simulink.

The simulation considers various input parameters, including the HTF mass flow rate, solar irradiation, ambient temperature, set-point temperature, and dry cooler air flow rate to regulate the cooling power. In line with the actual case, the simulation employs water as the circulating HTF with the same flow rate. Therefore, in comparing the numerical and experimental results,  $\Delta T$  realized by the solar field emerged as a comprehensive performance parameter.

Fig. 6 illustrates the comparison between the measurements and numerical results, focusing on the average HTF temperature  $T_{avg}$  (between the inlet and outlet of the field) and the  $\Delta T$  achieved by the field. The numerical results tend to overestimate the  $\Delta T$  and the  $T_{avg}$  provided by the solar field. Moreover, when examining the trend of  $T_{avg}$ , significant differences are observed primarily at the beginning and end of the day, during the warming up of the field. These differences can be attributed to variations in the exposure of collectors within a given array. For instance, the collectors mounted on the east side of the roof receive better illumination in the morning compared to those mounted on the west side.

The variations in collector exposure throughout the day introduce discrepancies in the heating and cooling of

the HTF, further emphasizing the need for separate monitoring of solar irradiation on each side of the roof.

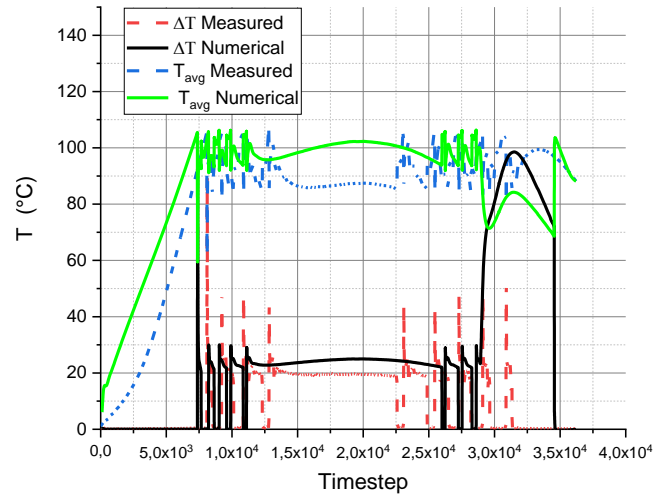


Figure 6 Measured  $\Delta T$  and the  $T_{avg}$  of the first experimental campaign carried out with single pyranometer configuration and comparison with simulation results.

### 3.2 Double pyranometer experimental configuration: measurement and numerical results.

Figure 7 displays the results obtained during the second measurement campaign on a specific day (9 July 2023). Solar irradiation was monitored using the double pyranometer configuration (fig.4). The set point temperature was maintained at 100 °C. The solar irradiation measurements were recorded from the east-facing pyranometer (G<sub>est</sub>) and the west-facing pyranometer (G<sub>west</sub>). In this case, the HTF flow rate, shown in Fig 7 a) in m<sup>3</sup>/h, is regulated to maintain the set-point temperature while providing a specific cooling power of the dry cooler. In fig. 7 b)  $P_{inc}$  represents the sum of solar power incident on collectors positioned on the east ( $G_{est} * A_c * N_{c-est}$ ) and the solar power incident on collectors mounted on the west facing side of the roof ( $G_{west} * A_c * N_{c-west}$ ). Fig. 8 illustrates the comparison between the measurements and numerical results; in this case, the simulation results differ from the experimental measurements by approximately 10 % versus the 25 % difference observed in the case of the previous experimental configuration. Looking at the trend of  $T_{avg}$  in Fig. 8, it can be noticed how numerical  $T_{avg}$ , calculated using the incident power reported in Fig. 7a), reproduces the measured HTF heating curve at the beginning of the acquisition.

Also, the oscillations observed after the solar field has reached the operating temperature are sensibly

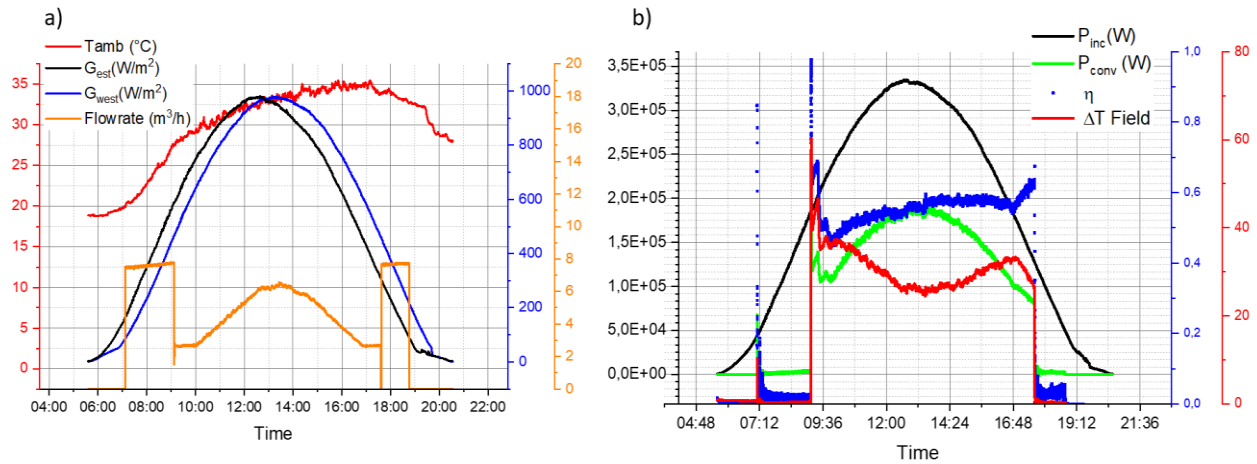


Figure 7 a) 9/07/2023 acquired weather data, and flow rate b) Measured field performance parameters with a set point temperature equal to 100 °C.

reduced, highlighting the importance of considering the different illuminations of collectors. In the analyzed HVFPC field operating at 95 °C, the measurements revealed a daily average conversion efficiency of 56% under an average irradiation of  $G_{avg}=650 \text{ W/m}^2$ . These results are considered, especially when compared to the findings in reference [8]. In that study, an 800 m<sup>2</sup> solar thermal plant coupled to a District Heating system in Geneva was monitored for over a year. The solar field comprised 400 MT-Power collectors and achieved a yearly efficiency of 46.4% with an average operating temperature above 80°C.

These findings indicate that the HVFPCs in the analyzed field are highly efficient and capable of generating significant thermal energy output even under varying irradiation conditions.

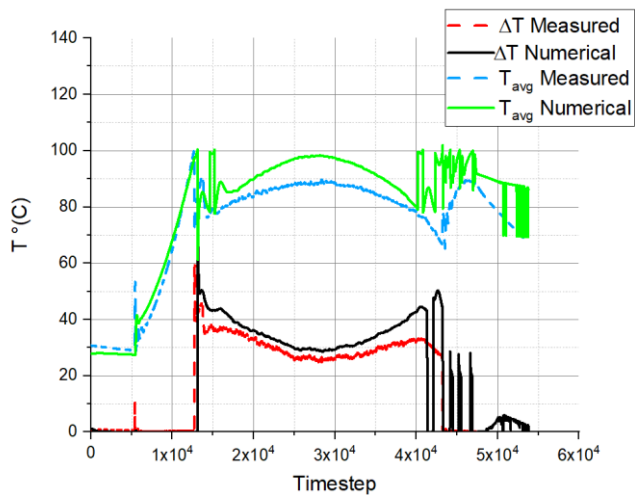


Figure 8 Measured  $\Delta T$  and the  $T_{avg}$  of the second experimental campaign carried out with double pyranometer configuration and comparison with simulation results.

#### 4. CONCLUSIONS

The performance of a thermal solar field composed of HVFPCs has been measured using two different experimental configurations. The field was assembled on the TVP Solar company building roof, adhering to the existing architecture, with its two sides facing east and west, inclined at 6° relative to the horizontal plane. The measurements taken considering the acquisition of only one pyranometer resulted in an underestimation of the field's efficiency. The measurement campaign was repeated using a second configuration involving two pyranometers positioned on both sides of the roof where the field is installed. The new measurements resulted in an efficiency value of 56% for the field when  $(T_{avg}-T_{amb})$  equals 60 °C.

The second campaign experimental measurement results differ by only 10% from numerical results obtained from a simulation model of the solar field implemented in Simulink instead of the 25 % difference observed in measurements carried with the single pyranometer configuration. Further analysis will be performed to improve the agreement between simulations and measurements and correctly predict the solar field energy production yearly in configurations when the collector inclination is not ideal.

#### DECLARATION OF INTEREST STATEMENT

The authors declare that they have no known competing financial interests or personal relationships that could have appeared to influence the work reported in this paper. All authors read and approved the final manuscript.

## REFERENCES

- [1] Y. Lv, P. Si, X. Rong, J. Yan, Y. Feng, e X. Zhu, «Determination of optimum tilt angle and orientation for solar collectors based on effective solar heat collection», *Applied Energy*, vol. 219, pp. 11–19, giu. 2018, doi: 10.1016/j.apenergy.2018.03.014.
- [2] S. Aggarwal, R. Kumar, D. Lee, S. Kumar, e T. Singh, «A comprehensive review of techniques for increasing the efficiency of evacuated tube solar collectors», *Heliyon*, vol. 9, fasc. 4, p. e15185, apr. 2023, doi: 10.1016/j.heliyon.2023.e15185.
- [3] B. A. A. Yousef, A. Radwan, A. G. Olabi, e M. A. Abdelkareem, «Sun composition, solar angles, and estimation of solar radiation», in *Renewable Energy - Volume 1 : Solar, Wind, and Hydropower*, Elsevier, 2023, pp. 3–22. doi: 10.1016/B978-0-323-99568-9.00023-6.
- [4] S. Karatasou, M. Santamouris, e V. Geros, «On the calculation of solar utilizability for south oriented flat plate collectors tilted to an angle equal to the local latitude», *Solar Energy*, vol. 80, fasc. 12, pp. 1600–1610, dic. 2006, doi: 10.1016/j.solener.2005.12.003.
- [5] G. Sandhu, K. Siddiqui, e A. Garcia, «Experimental study on the combined effects of inclination angle and insert devices on the performance of a flat-plate solar collector», *International Journal of Heat and Mass Transfer*, vol. 71, pp. 251–263, apr. 2014, doi: 10.1016/j.ijheatmasstransfer.2013.12.004.
- [6] A. Caldarelli *et al.*, «Low emissivity thin film coating to enhance the thermal conversion efficiency of selective solar absorber in high vacuum flat plate collectors», *Thin Solid Films*, vol. 764, p. 139632, gen. 2023, doi: 10.1016/j.tsf.2022.139632.
- [7] D. Gao *et al.*, «Experimental and numerical analysis of an efficiently optimized evacuated flat plate solar collector under medium temperature», *Applied Energy*, vol. 269, p. 115129, lug. 2020, doi: 10.1016/j.apenergy.2020.115129.
- [8] R. W. Moss, P. Henshall, F. Arya, G. S. F. Shire, T. Hyde, e P. C. Eames, «Performance and operational effectiveness of evacuated flat plate solar collectors compared with conventional thermal, PVT and PV panels», *Applied Energy*, vol. 216, pp. 588–601, apr. 2018, doi: 10.1016/j.apenergy.2018.01.001.
- [9] «Mathworks Simulink <https://www.mathworks.com/products/simulink.html>».
- [10] A. Duret, X. Jobard, G. Demonchy, e S. Pauletta, «Performance Monitoring of an 800m<sup>2</sup> Solar Thermal Plant with Evacuated Flat Plate Collectors Coupled to a DHN», *Eurosun 2022 Proceedings*, Eurosun 2022 Proceedings, 2022.